Science of the Total Environment 817 (2022) 152992

Contents lists available at ScienceDirect

Science of the Total Environment

journal homepage: www.elsevier.com/locate/scitotenv

Local flow convergence, bed scour, and aquatic habitat formation during floods around wooden training structures placed on sand-gravel bars

Sohei Kobayashi [a,*], Sameh A. Kantoush [b], Mahmood M. Al-mamari [b], Masafumi Tazumi [b], Yasuhiro Takemon [b], Tetsuya Sumi [b]

[a] College of Life and Environmental Sciences, Wenzhou University, Wenzhou, Zhejiang 325035, China
[b] Disaster Prevention Research Institute (DPRI), Kyoto University, Gokasho, Uji, Kyoto 6110011, Japan

HIGHLIGHTS

- Flow behavior around river training structures were monitored by UAV during floods.
- Flow was diverted and converged due to the structures in partially submerged floods.
- The ponds developed by bed sours around the structures on a bar after the floods.
- The ponds were filled by sand and dewatered after fully submerged floods.
- Water temperature fluctuation was smaller for the ponds than river main flow.

GRAPHICAL ABSTRACT

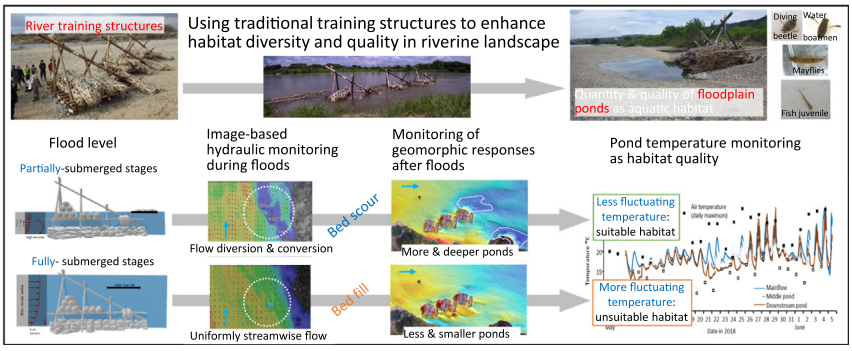

ARTICLE INFO

Article history:
Received 8 September 2021
Received in revised form 4 January 2022
Accepted 5 January 2022
Available online 10 January 2022

Editor: Ashantha Goonetilleke

Keywords:
Gravel bars
River training structure
Scour holes
LSPIV
Submergence
Water temperature

ABSTRACT

Riverine ponds, which are formed and sustained through sediment erosion and deposition, are key habitats for enhancing biodiversity in river reaches. The objective of this study was to understand the roles of traditional river-training wooden structures called "seigyu" on the formation of ponds on nonvegetated bars. Here, the spatial and temporal patterns of the flow and bedform coupled with pond formations for several flood events were assessed. The surface flow patterns were monitored by an unmanned aerial vehicle (UAV) and evaluated by large-scale particle image velocimetry (LSPIV); the maximum flow velocities were 1.3 m s^{-1} and 1.9 m s^{-1} during floods when seigyu units were partially and fully submerged, respectively. Although the overall mean flow velocity was greater for the latter events, the spatial variation in flow velocity and dissipation rate of turbulent kinetic energy (TKE) around seigyu was greater for the former events. Such flow patterns affected both bed formation and ecological habitats; ponds were formed at locations beside and behind seigyu, where the flow converged and bed scouring occurred during floods. The frequency and size of ponds around seigyu increased in the early half of the season, and they decreased in the other half when floods were greater in magnitude, which suggests that the bed scouring effect of seigyu was greater in flood stages with partial than fully submergence. Although the bar ponds lack shade to temper the effects of incident light and atmospheric conditions, the ponds displayed smaller daily oscillations in temperature than did the main river, probably due to hyporheic water supply to the ponds. Because many aquatic species cannot tolerate extremely high temperatures in summer, the generation and maintenance of deeper ponds by scouring with sufficient water exchange with the hyporheic zone can be key to enhancing colonization by various aquatic species.

* Corresponding author.
E-mail addresses: koba@wzu.edu.cn (S. Kobayashi), kantoush.samehahmed.2n@kyoto-u.ac.jp (S.A. Kantoush), almamari.mahmood.78c@st.kyoto-u.ac.jp (M.M. Al-mamari), takemon.yasuhiro.5e@kyoto-u.ac.jp (Y. Takemon), sumi.tetsuya.2s.2s@kyoto-u.ac.jp (T. Sumi).

http://dx.doi.org/10.1016/j.scitotenv.2022.152992

1. Introduction

Bedforms with moderate spatial amplitudes of sediment, such as pool-riffle sequences, are indispensable for promoting the diversity of aquatic habitat and biota within river reaches (Kani, 1981; Huryn and Wallace, 1987; Poole, 2002). Habitats are defined here as local areas with certain bed and flow conditions, such as pools and riffles (i.e., lotic habitats in main flow), backwaters or side arms (semilentic habitats that are partly connected to main flow) and floodplain ponds (fully lentic habitats that are completely isolated from main flow) within river reaches (Frissell et al., 1986; Hawkins et al., 1993; Amoros, 2001). These habitats are formed, modified, and deformed by flow variability, erosion and deposition of sediments, which are influenced by the magnitude and characteristics of floods, the quantity and quality of available sediment, and the existence of flow obstructions.

Boulders, large woody debris, river training structures (e.g., spur dykes, deflectors), and certain types of weirs play key roles in the formation and maintenance of habitat structures within river reaches (Carré et al., 2007; Nagayama and Nakamura, 2010; Roni et al., 2015). These in-channel structures can promote local erosion on one side and deposition on the other side by increasing the spatial variations in 3-dimensional hydrodynamics and morphodynamics during different flood events. Large woody debris, which is installed in a structured-anchored or an unstructured-unanchored manner in channels, has often been used for the restoration of pools and riffles for invertebrates and fish in small streams (Nagayama and Nakamura, 2010; Roni et al., 2015). In addition, spur dykes consisting of cobbles and other hard materials are often used in habitat rehabilitation in lowland streams and rivers (Carré et al., 2007; Zhang and Nakagawa, 2008; Pandey et al., 2017). Although many studies have reported bedform and biological responses to implemented training structures, few studies have coupled and monitored flow and morphological patterns during floods, as well as the resulting geomorphic responses. In particular, the responses of habitats to floods of different magnitudes have not been well explored.

Riverine ponds are in-channel water bodies isolated from the main flow except during floods. Even though such ponds cover a small portion of the aquatic area, because they offer lentic habitats in totally lotic systems (i.e., rivers), they are often a key to increasing biodiversity in river reaches (Harper et al., 1997; Zilli and Marchese, 2011; Couto et al., 2018). These ponds occur near the main flow, such as gravel bars and frequently inundated side flow paths, which are cross-sectionally lower elevation and active part of the channel. Ponds also form at a distance away from the main flow in old and abandoned flow paths in alluvium terraces, which are often at relatively higher elevations in the channel, inactive, and vegetated. According to the distance from the main flow and elevation, ponds differ in their flow inundation regimes and thus connectivity and flow disturbance characteristics, which affect water and bottom quality, the surrounding vegetation, supply of organisms from the main flow, basal food, and faunal community (Tockner et al., 1998; Amoros and Bornette, 2002; Karaus et al., 2005; Zilli and Marchese, 2011; Van den Brink et al., 2013). Closely located ponds can also vary in depth, surface area, and source of water, thus influencing water quality and the inherent aquatic community (Feyrer et al., 2004; Nhiwatiwa et al., 2011). Irrespective of the location in the channel, ponds form in locally depressed (i.e., concave bed) areas. Thus, ponds are generated and maintained at locations where flow converges, and bed scour occurs in the proximity of flow obstructions such as boulders, large woody debris, protruded alluvium areas or bank-protecting structures. The decrease in abundance and degradation of riverine ponds are evident in many rivers worldwide due to reductions in flooding following the construction of upstream dams and the prevention of lateral flow by levees (Gergel, 2002; Bowen et al., 2003; Skern et al., 2010). The decoupling of main flow and floodplain areas due to channel degradation (i.e., active channel incision) is often evident (Choi, 2014; Negishi et al., 2014), which was attributed to reduced sediment transport by excavation projects and the establishment of upstream dams (Kondolf, 1997; Nakamura et al., 2017).

Riverine ponds are fed by hyporheic water, groundwater, or surface runoff after rainfall (Amoros and Bornette, 2002; Karaus et al., 2005). The hydrological characteristics of ponds are considered to be greatly affected by the subsurface water level in the floodplain, which is linked with the water level of the main river. In case of bare bars close to the main flow, temporary or semiperennial ponds can be sustained by hyporheic water, which originates from river surface water that enters the sand or gravel layer upstream of the bars (Burkholder et al., 2008; Ock et al., 2015; Trauth et al., 2015; Dole-Olivier et al., 2019). These ponds are likely to occur as long as the bottom of depressed areas is below the subsurface (hyporheic) water table. In addition, residence time and thermal stability are generally greater for deeper hyporheic water (Briggs et al., 2012; Gariglio et al., 2013; Marzadri et al., 2013; Cranswick et al., 2014). Thus, the depth of depression is assumed to be a determinant of the longevity and thermal conditions of these ponds, which in turn determine the habitat quality of these ponds for aquatic organisms.

This study is a part of an ecosystem restoration project that adopted traditional river engineering works to improve the habitat quality in a lowland reach of the Kizu River in Japan. The river is one of the Japanese rivers that have experienced severe channel degradation since the 1960s, and historical decreases in overall habitat diversity, the number of floodplain ponds, and lateral connectivity have been reported (Choi, 2014; Choi et al., 2018b). Timber frame structures named "seigyu" had been used to promote sediment deposition and mitigate bank erosion during severe floods in Japanese rivers (Tomino, 2002). However, the use of seigyu was replaced by the installation of modern grey structures (concrete engineering works) to improve resistance and decrease construction costs in the middle of the 20th century. For a revival of nature-based solutions and traditional techniques, the restoration project focused on some of the advantages of seigyu structures in river ecosystems; they consist of nature-friendly materials such as timber, bamboo, and stones and are unanchored, which allows them to acclimate to local hydraulics and beds. Three seigyu units were installed on a sand-gravel bar in the first year of the project that intended 1) to divert flood flow to both banks, which promoted the erosion of the vegetated banks, 2) to increase connectivity between the main flow and ponds on an elevated terrace, and 3) to increase the ponds by local erosion and deposition around seigyu. The geomorphological responses of the bar and biological features of ponds were reported by Tazumi et al. (2019).

The objective of this study is to analyse the effects of the installed series of seigyu structures on the formation of bar ponds (i.e., ponds that occur in bare bars) during several flood events in which the seigyu units were partially and fully submerged. The detailed characteristics of the Kizu River and seigyu units are described in the following section. Field measurements, including those obtained with an aerial monitoring technique by UAV (unmanned aerial vehicle), large-scale particle image velocimetry (LSPIV), and array of propeller-type current meters during selected floods, were collected to investigate the hydromorphodynamics of newly formed ponds with different geometries and extents. Finally, by monitoring the water temperature in selected ponds, geomorphic influences on the water temperature, as a quality of habitats for aquatic fauna, were discussed.

2. Study site and methods

2.1. Channel degradation history for the river

The study was conducted on a lower reach (15 km upstream from the confluence) of the Kizu River (watershed: 1596 km^2), a tributary of the Yodo River in western Japan (Fig. 1a, b). The Kizu River, especially the lower reaches, was sandy due to weathered granite in the upstream area. There were a total of 5 dams, Takayama (constructed in 1969), Shourenji (1970), Murou (1974), Nunome (1992), and Hinachi (1999), in the upstream basin.

The largest floods (recurrence: >5–10 years) were nearly 6000 $m^3\ s^{-1}$ before the construction of the Takayama Dam; however, they decreased to 3000–4000 $m^3\ s^{-1}$ after the construction of the dam (Choi, 2014). The estimated amount of bed-load transportation downstream of the dam

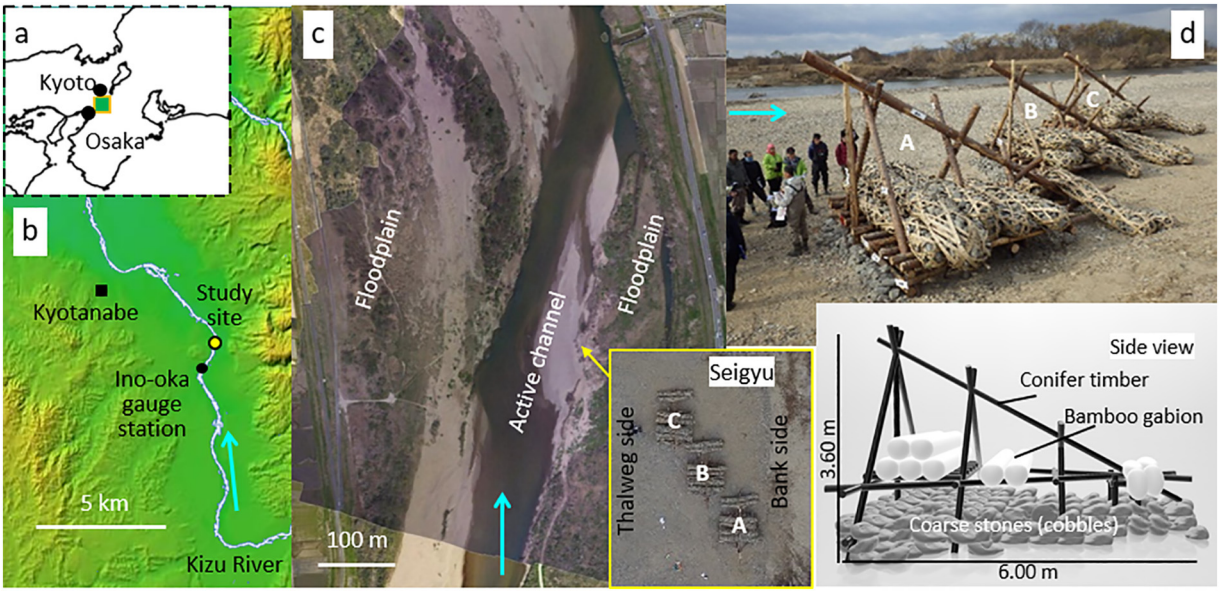

Fig. 1. Maps of the Kansai region (a), lower Kizu River (b), and study reach (c) and photo of the seigyu structures after installation in December 2017 (d). The seigyu units were named A, B, and C from upstream to downstream. Blue arrows show the flow direction. The map in (b) was based on products from the Geospatial Information Authority of Japan.

decreased from approximately 183,000 m^3 y^{-1} in the 1960s to 23,000 m^3 y^{-1} in the 2000s (Choi, 2014). In addition, excavation was performed in the lower reaches of the Kizu River and in the main Yodo River until the 1970s. The riverbed elevation decreased more than 2–3 m from the 1960s to 2010s throughout the lower 26 km reaches of the Kizu River. The channel degradation and reductions in flood intensity led to a transition from a braided channel to a single or alternating channel. In addition, the growth of vegetation was promoted on terraces, likely due to the reduced frequency of inundation. The reductions in flood inundation and disturbances also deteriorated riverine ponds in terms of habitat quality and quantity (Choi, 2014; Choi et al., 2018a, 2018b).

2.2. Target reach and training structures

The survey reach in the Kizu River was 15.2 km upstream from the confluence of the Yodo River (Fig. 1b, c). The channel width was 450 m, and the channel slope was 1/1000. The mean annual maximum discharge, which corresponded to bankfull discharge, was approximately 2000 m^3 s^{-1}. The active channel width was 110–140 m, and the flow width was nearly half of the active channel width under low-flow conditions (<30 m^3 s^{-1}). A sand-gravel bar was located on the right-bank side of the main river. The surface materials were mainly sand (0.25–2 mm) and gravel (2–16 mm), but pebbles (16–64 mm) appeared sporadically. The bar was submerged when the discharge was greater than 150 m^3 s^{-1}.

Three seigyu units were constructed on the bar close to the right bank of the active channel in December 2017 (Fig. 1c, d). Each unit consisted of wooden piles (logs) with a triangle pyramid shape; their dimensions were 6.0 m long, 4.0 m wide, and 3.6 m high (middle-sized type seigyu, Tomino, 2002) (Figs. 1d, S1). To deflect flow, the three units were placed in a line with an angle directed to the left bank downstream (Fig. 1c). To protect sill erosion around each unit, coarse stones larger than pebbles were overlaid on the bed near the wooden bases. They were unanchored and permeable structures. To maintain the stability, 9 bamboo gabions (cylindrical shape, diameter: 0.5 m, length: 4 m) with plenty of stones inside were laid on the wooden base. Such nature-based structures work differently than modern engineered structures, as they change their characteristics to acclimate to local hydraulics and beds. The seigyu units were named A, B, and C sequentially from upstream to downstream (Fig. 1c, d).

2.3. Hydromorpho-dynamic measurements by UAV

Water level and discharge data were available at the Ino-oka gauge station (Fig. 1b), which was 1 km upstream from the study reach. A geomorphic survey around the seigyu units was conducted in 6 nonflood periods when the flow was low and the bar surface was completely dry, except in bar ponds. A flow survey around the seigyu units was conducted during floods at a discharge of approximately 250 m^3 s^{-1} on the 9th of May and at 1200 m^3 s^{-1} on the 29th of July (Fig. 2a). The former was a controlled flood or environmental flushing flow released by the upstream Takayama Dam, and the latter occurred during a typhoon event. In the former event, one-third of the seigyu units were submerged, and in the latter, they were fully submerged (only a protruded driftwood trapped by seigyu B was visible above the water surface, Fig. 2b).

To obtain topographic features, aerial images and videos were recorded using DJI Phantom 3 (DJI Japan, Tokyo, Japan), whose flight area covered the target bar. A photo was captured 50 m above the ground every 5 s so that two consecutive photos overlapped by more than 50%. A digital elevation model (DEM) and orthogonal map of the bar were obtained through image processing with motion photogrammetry using Metashape (Agisoft

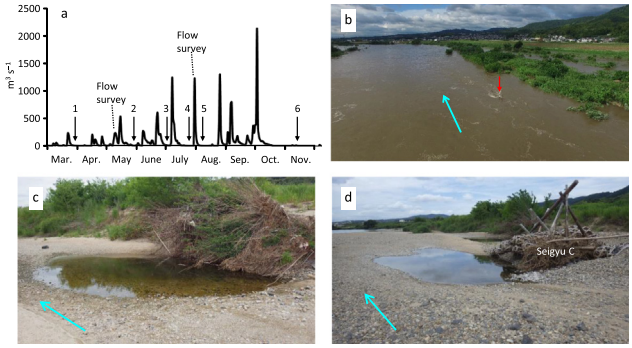

Fig. 2. Flow discharge pattern in 2018 at the Ino-oka gauge station and an angle view during the second flow survey (only a protruded driftwood trapped by seigyu B, red arrow, was visible). The numbers in hydrograph denote the period of the pond survey during low flows. The blue arrow shows the flow direction.

LLC, St. Petersburg, Russia). Dense cloud points were used to generate a DEM with a 0.1-metre resolution for ambient seigyu units, and the DEM was scaled and georeferenced based on ground control points and overlapping images to identify matching points.

Stable and suitable videos in plan view were captured for the surface flow patterns during the two floods with the UVA in intelligent flying mode, which is suitable for imaged-based analyses of LSPIV (Almamari et al., 2019). The videos were taken 35–50 m above the water surface. The original frame rate of videos was 25 fps at a resolution of 4096 × 2160 pixels. Pairs of images were extracted from videos and processed in Dynamic Studio software (Dantech Dynamics, Skovlunde, Denmark); the size of the investigated area was 32 × 32 pixels, and 50% overlap was used to measure the velocities around seigyu. The selected image sequence was rescaled based on the real geometry between point pairs present in the field of view. Averaged image pairs of 199 and 301 frames were used to compute the surface flow velocity for partially and fully submerged conditions, respectively.

To validate the flow estimated by LSPIV, the flow around seigyu was measured in the field during the first flood. The safety of workers around the seigyu units was ensured during the controlled (planned hydrograph) flood. The surface flow velocity was measured using a VR-301 propeller-type current meter (Kenek Corporation, Tokyo, Japan), and the flow direction was determined visually at 8 positions around each seigyu unit (a total of 24 locations).

2.4. Flow turbulence calculation based on LSPIV results

The surface flow velocity at a given point fluctuates with time associated with eddying, swirling, and upwell motions of water. The turbulence patterns in the presence of seigyu structures at different flood events were evaluated through turbulent kinetic energy (TKE) and its dissipation rate based on LSPIV data. The TKE is characterized by the variance of flow velocity around the mean.

$$TKE = \frac{\sigma_u^2 + \sigma_v^2 + \sigma_w^2}{2} = \frac{0.5}{N-1}\sum\left[(u_n - \overline{u})^2 + (v_n - \overline{v})^2 + (w_n - \overline{w})^2\right]$$

where σ is the standard deviation, u, v, w are streamwise, transverse, and vertical components of flow, respectively, subscript n and bar are the instantaneous and mean flow velocities, respectively, and N is the number of instantaneous velocities in the time series from LSPIV calculated vector maps. The dissipation rate of TKE has been used to estimate bed shear stress from LSPIV data (Johnson and Cowen, 2017). The surface dissipation rate of TKE (ε) was calculated based on the large eddy PIV method proposed by Sheng et al. (2000) and applied by Jin and Liao (2019).

$$\varepsilon = -2\tau_{ij}\overline{S}_{ij}$$

where τ_{ij} is the shear stress tensor obtained from the measured 2D surface velocities based on the Smagorinsky model and S_{ij} is the strain rate tensor (Jin and Liao, 2019). The time series of the instantaneous velocities in the streamwise and transverse directions were used to calculate TKE. The flow velocity magnitude, TKE, and dissipation rate of TKE were visualized and analysed by using an in-house tool written in MATLAB.

2.5. Pond occurrence and water temperature

The occurrence of ponds on the bar was surveyed, and the water depth and area of each pond were measured over 6 non-flood periods when the flow was low (Fig. 2a, c, d). Depth was measured using a steel scale at the deepest point. The surface area of each pond was measured based on the length of the long axis and over 3–5 cross-sections.

Water temperature was recorded in two bar ponds and in the main flow using a pendant-type logger (HOBO UA-002-64, Onset, Bourne, USA) from the 9th of May to the 5th of June 2018. The logger was bound to a stone and placed at the middle of ponds or a few steps inside the main flow. Temperature was recorded every 10 min. The connection of the main flow and ponds during periods of increased water level was recorded based on images taken by time-lapse cameras (TLC200, Brinno, Taipei, Republic of China) every 30 min during the measurement period. Air temperature data during the survey were collected from the nearest monitoring station (Kyotanabe, Fig. 1b) of the Automated Meteorological Data Acquisition System (AMeDAS).

3. Results

3.1. Validation of LSPIV estimated flow velocity

The spatial variation in the mean flow velocities estimated by LSPIV reasonably agreed with that actually measured in the field (Fig. 3). The time-averaged velocity from time series of the instantaneous velocities was used to show the LSPIV result. In both methods, the mean flow velocity was the highest at positions 1 and 2, the front and thalweg (i.e., river middle) sides of seigyu, for all seigyu units, and the downstream unit (seigyu C) displayed the highest velocity at these positions (Fig. 3a, b). At positions between the front and back sides of each seigyu (positions 2–8), the mean flow velocity was less than 0.5 m s^{-1}, except at position 4, which corresponds to a narrow space between two seigyu units or between seigyu and the bank. The coefficient of determination for the flow velocities between the two methods was high and significant ($R^2 = 0.856$, $p < 0.001$) (Fig. 3c). Therefore, the flow velocity estimated by LSPIV was ensured to be reliable enough for analysing the spatial patterns of the surface flow velocity.

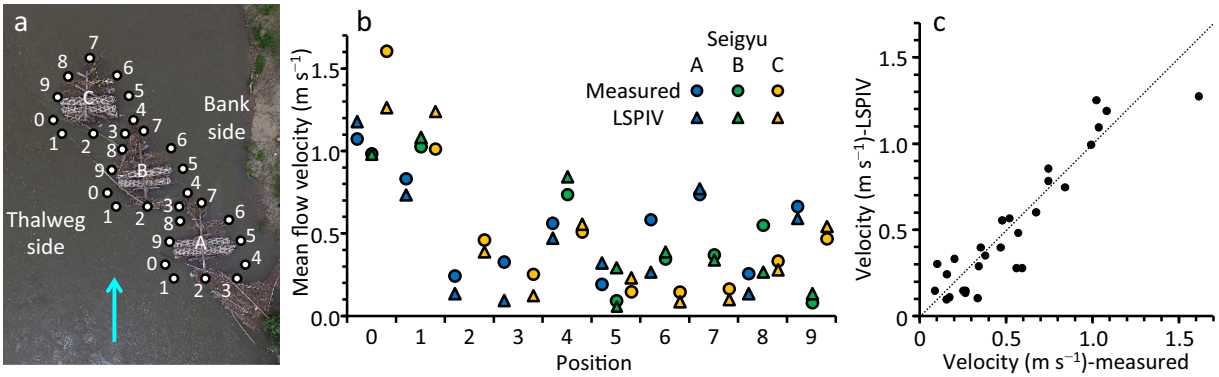

Fig. 3. Positions of flow measurements (a), field-measured and LSPIV-estimated mean flow velocities at each position ordered counterclockwise for each seigyu (b), and relationship between the measured and LSPIV-estimated flow velocities (with a line of equality). The blue arrow shows the flow direction.

3.2. Flow patterns during floods

Riverbed evolution is coupled with variations in flow patterns, water level and sediment transport. The flow characteristics around the seigyu structures at two different flood levels (i.e., partially and fully submerged conditions) are comprehensively shown in Fig. 4; ten cross-sections of surface flow velocities (time-averaged flow velocities) were derived from LSPIV analysis to evaluate surface flow behavior (Fig. 4a–d).

In the partially submerged condition, the flow velocity was substantially reduced, and the flow diverged at the seigyu locations, as is evident in the 2D flow velocity distribution map (Fig. 4a) and the cross-sectional flow profile (Fig. 4b). At cross sections 3–8, continuous zero velocity can be clearly observed corresponding to the location of the seigyu, where flow was hindered by the wooden piles and separated vertically to near-bed flow below the seigyu and near the upper gabions. The upper flow velocity was reduced as the flow passes through the permeable part of each unit, with a small recirculation zone behind each seigyu. The velocity sharply increased at the thalweg (river middle) side of seigyu from 0 to more than 0.6 m s^{-1} at cross-section 3 (seigyu A), to nearly 1.0 m s^{-1} at cross-section 5 (seigyu B) and to more than 1.2 m s^{-1} at cross-section 7 (seigyu C). The velocity also sharply increased at the bank side of each seigyu unit at cross-sections 3–8, although the value was almost half of that at the thalweg side of seigyu. Such sharp changes in flow around seigyu units suggest potential areas for energy dissipation where erosion and deposition occur.

The group of three installed seigyu units formed an extended buffer zone aligned in the streamwise direction, and the surface flow velocities were significantly reduced, as shown by the blue band in the map (Fig. 4a) and as a large depression in cross-sections 3–10 (Fig. 4b). This zone acts as a sponge that alters the approaching flow. Hence, seigyu units separated and accelerated the flow towards the river middle and right bank. The length of the buffer zone extended almost 100 m in the streamwise direction and 50 m in the transverse direction.

In contrast, in the fully submerged condition, only protruding driftwood (approximately 10 cm higher than the top of seigyu) trapped by seigyu B was visible, with reduced flow velocity around it (Fig. 4c, d, cross-section 5). The flow velocity in the middle zone was 1.6–2.0 m s^{-1} and was apparently higher than that in the partially submerged condition. Although the flow velocity continuously decreased from the thalweg to bank side of seigyu in each section, there was no drastic change in velocity. Thus, despite the comparatively high velocities, there was no apparent evidence of flow diversion or conversion near seigyu units in this condition. A weak buffer zone, shown as a green band expanding downstream (Fig. 4c) and as a gentle slope in cross-sections 3–10 (Fig. 4d), was visible due to the presence of seigyu. The length of the zone was almost 200 m in the streamwise direction and 100 m in the transverse direction.

In summary, the flow variation near the seigyu units and the occurrence of a clear buffer zone indicate that the effect of seigyu units on surface flow patterns was greater for the partially submerged condition than for the fully submerged condition. In the partially submerged condition, the

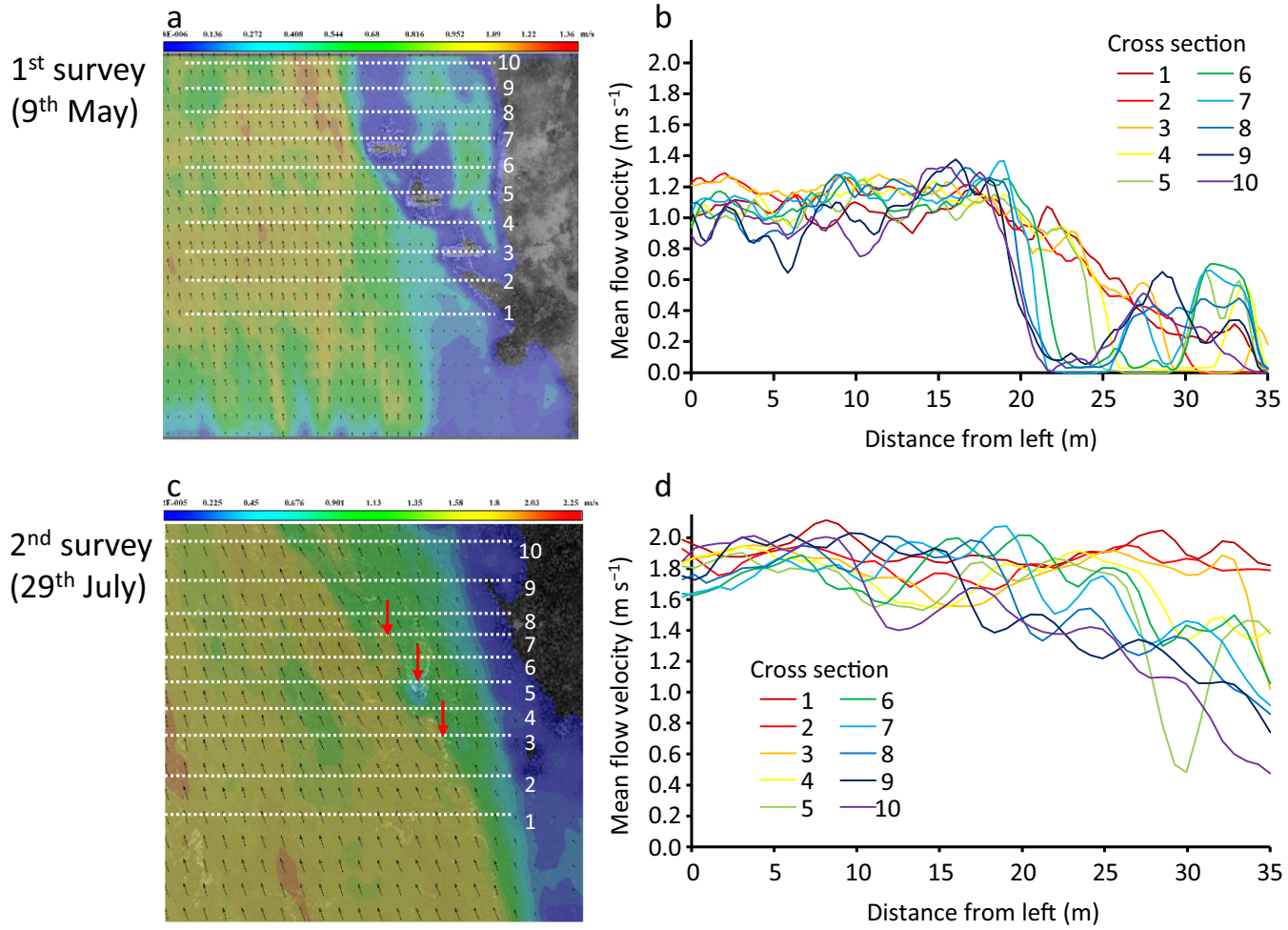

Fig. 4. Surface flow pattern near the seigyu units determined by LSPIV during the 1st (a, b) and 2nd (c, d) surveys. Spatial distributions of the mean flow velocity and direction (a, c), and flow velocity profiles along ten cross-sections (c, d). Red arrows show the approximate positions of the three seigyu units in the 2nd survey.

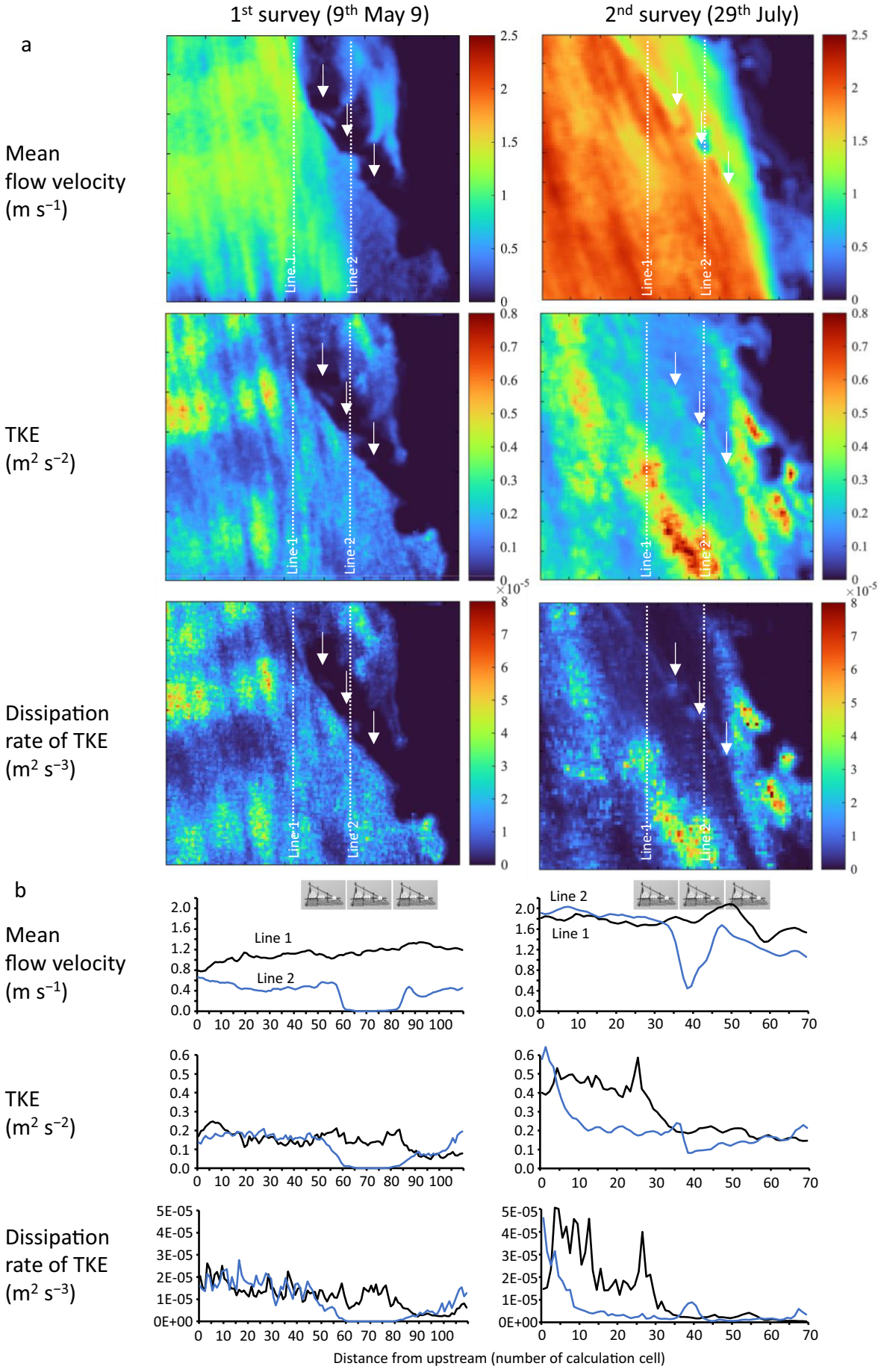

(caption on next page)

approaching flows with high velocities hit the structures and entered a downstream mixing zone with low flow velocities. When the flow travels from the first unit towards the subsequent units, a small recirculation flow field was created. Energy dissipation can occur in such zones, resulting in erosion and deposition.

3.3. TKE and dissipation rate of TKE

TKE and its dissipation rate are shown in 2D maps (Fig. 5a) and as profiles along selected lines (Fig. 5b) together with the mean flow velocity (same results as Fig. 4) for the partially and fully submerged conditions. Although the TKE was higher overall for the fully than partially submerged condition, similar TKE values were observed near seigyu units between the two conditions. The TKE tended to be high where the mean flow velocity varied spatially, such as the upstream part between the two lines and near the bank in the fully submerged conditions (Fig. 5a). The TKE values of nearly 0.2 $m^2\ s^{-2}$ were observed at the thalweg (river middle) side of seigyu B and C (line 1 of Fig. 5b) and downstream of seigyu C (line 2 of Fig. 5b) for both conditions. Higher TKE values possibly due to the presence of the seigyu units were not evident in the maps, except the downstream bank side of seigyu C in the partially submerged condition. In fully submerged condition, the TKE was exceptionally high between the seigyu A and bank with an overhanging tree.

The dissipation rate of TKE showed a spatial distribution similar to that of TKE under both conditions. However, the difference from TKE was evident by higher dissipation rates in the partially submerged condition than in the fully submerged condition, especially around the seigyu units (Fig. 5a). The dissipation rate was more than $1.0 \times 10^{-5}\ m^2\ s^{-3}$ at the thalweg side of seigyu B and C (line 1 of Fig. 5b) and the downstream seigyu C (line 2 of Fig. 5b) in the partially submerged conditions, while it was far below $1.0 \times 10^{-5}\ m^2\ s^{-3}$ at the same locations in the fully submerged conditions. In fully submerged condition, the dissipation rate of TKE was exceptionally high between the seigyu A and bank.

In summary, TKE and its dissipation rate were evaluated to understand surface flow turbulence. Increased TKE and its dissipation rate, possibly due to the existence of seigyu units, were not evident except downstream of seigyu C in the partially submerged condition. The TKE around seigyu was similar between the two conditions, while its dissipation rate, which potentially relates to bed shear stress, around seigyu was higher in the partially than fully submerged condition.

3.4. Bed and pond responses around seigyu units

In period 1, the bed near the seigyu units was flat with a gentle up- to downstream gradient, and there was no pond near the seigyu units (Fig. 6a). In period 2, a depressed area was evident at the thalweg (river middle) side of seigyu C, where a pond occurred for the first time near seigyu (Fig. 6a), as a consequence of local erosion between periods 1 and 2 (shown by blue, Fig. 6b) with a partially submerged flood in May. Local deposition (shown by yellow and red, Fig. 6b) was also evident behind seigyu C (in a streamwise manner) and behind the depressed area. The depressed area became increasingly deeper and wider in period 3 due to the local erosion between periods 2 and 3 with a partially submerged flood in June. A few small, depressed areas without ponds (i.e., no surface water) also occurred around seigyu B. In period 4, small ponds were evident in front of seigyu A and nearby (thalweg and back sides of) seigyu B, where the local erosion occurred between periods 3 and 4 with a fully submerged flood in early July. Meanwhile, the pond at the thalweg side of seigyu C was partially filled, and the pond next to the natural bank, which was the largest of all ponds in periods 1–3, was fully filled. In period 5, all previous ponds were partially or fully filled due to deposition near and upstream of seigyu units between periods 4 and 5 with a fully submerged flood at the end of July. The two fully submerged floods in July (occurring before period 4 and period 5) had almost the same peak discharge, but they differed in the recession stage (i.e., discharge decreased sharply in the latter flood, Fig. 2a) and the erosion-deposition pattern. Three floods occurred after period 5, and we did not have a chance to visit during low flows for three months. In period 6, after the maximum flood of this year, all previous ponds were filled. Between periods 5 and 6, deposition occurred widely both upstream and downstream of the seigyu units except between the seigyu A and bank with an overhanging tree, where marked erosion occurred (Fig. 6b).

In summary, local erosion occurred and ponds developed nearby the seigyu units more in the early half of the study periods associated with partially submerged floods, while deposition occurred widely nearby and upstream of the seigyu units more in the latter half associated with fully submerged floods. The greater erosion in the partially than fully submerged floods did not correspond to the lower flow velocities in the former floods, but it corresponded to the higher dissipation rate of TKE around seigyu. Meanwhile, the exact locations of erosion around the seigyu units in the partially submerged floods corresponded more to the spatial patterns of the mean flow velocity than to the dissipation rate of TKE.

3.5. Frequency and depth of ponds

Ponds around natural banks occurred since period 1, whereas ponds around seigyu units occurred since period 2. The frequency of ponds (i.e., number of ponds that occurred in the bar) increased from 2 to 5 between periods 1 and 2 (Fig. 7a) with a partially submerged flood in May. The frequency did not change between periods 2 and 3 with a partially submerged flood in June, whereas the surface area and depth of each pond increased (Fig. 7b, c). The frequency of ponds increased from 5 to 8 between periods 3 and 4 with a fully submerged flood of early July, with the size of all the ponds near seigyu increasing. However, the frequency of ponds decreased from 8 to 6 between periods 4 and 5 with a fully submerged flood at the end of July, and it further decreased to 3 in period 6 after the maximum flood of this year occurred in October. The size of ponds also decreased after period 4; ponds that exceeded 5 m^2 in surface area and 10 cm in depth, which constituted half of all ponds in periods 1–4, were not observed in period 5.

There was a positive relationship between the surface area and depth of ponds (power function model, $n = 30$, adjusted $R^2 = 0.382$, F-statistic $= 18.94$, $p < 0.001$; Fig. 7d). In the biplot of surface area and depth, many seigyu ponds were plotted on the upper side of the fitted curve, which suggests that seigyu ponds tended to be deep for a given surface area.

3.6. Water temperature of ponds

Ponds sometimes exhibited large deviations in water temperature and the diel oscillation pattern compared to those of the main flow (Fig. 8a, b). When ponds were connected to the main flow, for example, during the increased water level period from the 14th to 20th of May, ponds exhibited temperature and diel cycles similar to those of the main flow. When the ponds were isolated from the main flow, for example, from the 21st to 25th of May, the average temperature and daily temperature range were lower for the ponds than for the main flow. However, with a further decrease in the water level, the surface water of the downstream pond was almost submerged in the bed from the 26th to 30th, and the recorded temperature fluctuated in a range close to the air temperature. The temperature and temperature range of the middle pond, which was deeper than the downstream pond, were continuously lower and smaller than those for the main flow. Stage-dependent responses of water temperature to air temperature are

Fig. 5. Two-dimensional spatial distribution (a) and profile along longitudinal lines (b) for the mean surface velocity, turbulent kinetic energy (TKE), and surface dissipation rate of TKE for partial and fully submerged conditions. Approximate locations of the seigyu units are shown by white arrows (a) and the schematic picture (b).

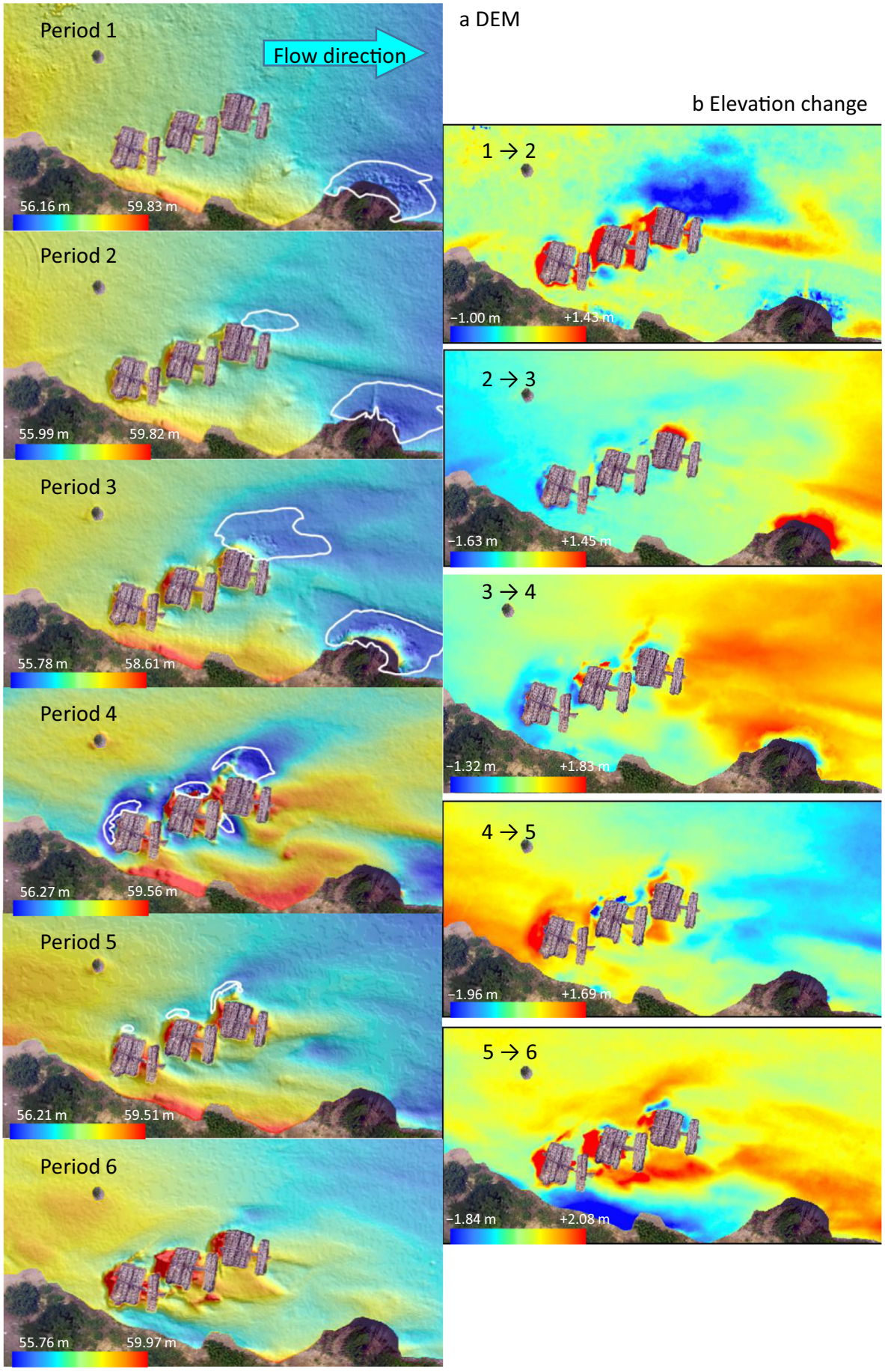

(caption on next page)

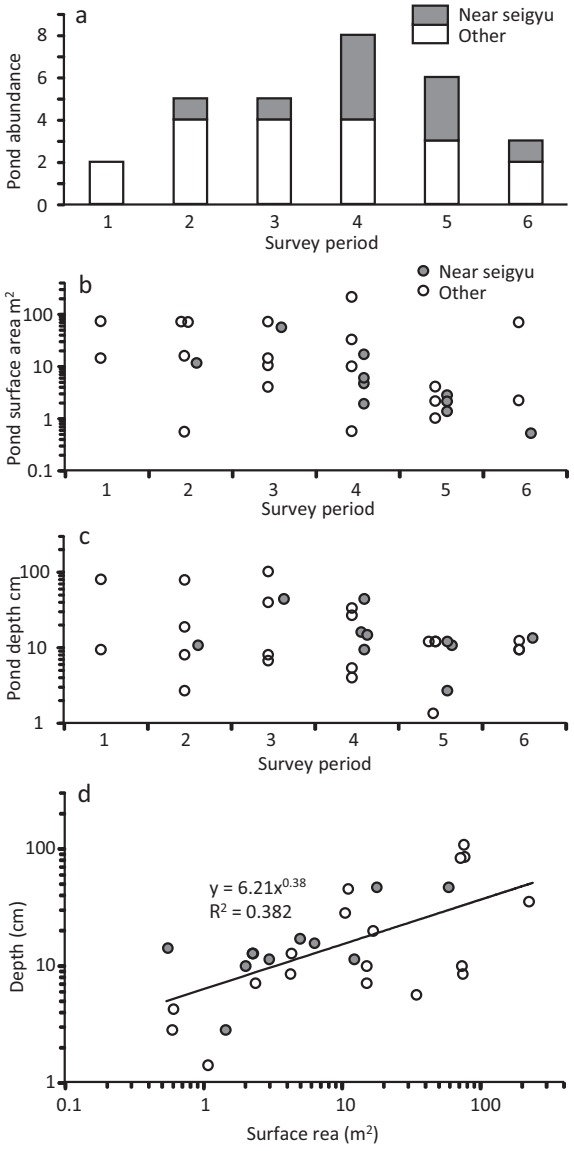

Fig. 7. Changes in the pond characteristics (a: frequency, b: surface area, c: depth) during the study and the relationship between the area and depth of all ponds throughout the survey (d).

also evident in the biplot of air and water temperatures (Fig. 8c). When ponds were connected to the main flow, water temperature varied less among the 3 water bodies and increased slightly with air temperature. When ponds were isolated, the water temperature and its slope with increasing air temperature were lower for ponds (especially the downstream pond) than for the main flow. When the downstream pond was dewatered, the water temperature of the pond increased with the air temperature, while the temperature of the middle pond showed a gentler increase with air temperature than that of the main flow.

4. Discussion

Our study demonstrated that seigyu river training structures and floods promoted the development of riverine ponds, an important riverine habitat for biodiversity, on sand-gravel bars. However, in contrast to our expectation, the number and size of ponds tended to decrease in the middle-to-late flood season, when larger floods were frequent. The surface flow patterns around the seigyu units during floods evaluated based on UAV monitoring and an LSPIV technique showed that although the mean flow velocity was low, spatial variations in flow and the occurrence of flow convergence were greater for the smaller flood when the seigyu units were only partially submerged. In addition, the dissipation rate of TKE, which could be associated with bed shear stress, around seigyu was greater in the smaller flood. These results suggest that the bed scouring effect of seigyu can be greater below a certain flood threshold than in the higher-flow stages. The water temperature of the two ponds and the main flow monitored during the nonflood period exhibited a daily cycle that changed depending on the water level stages and exhibited smaller oscillations in the ponds than in the main flow.

4.1. Water level and seigyu effects on pond formation

Ponds were developed in areas where flow converged due to the existence of seigyu units during floods. One such location was at the thalweg (river middle) side of the seigyu structures. Flows approaching upstream were diverted to the thalweg and bank sides of the seigyu (Fig. S2). One of the diverted flows at the upstream seigyu (seigyu A) soon converged to another approaching flow at the second seigyu (seigyu B). Accordingly, flow at the thalweg side cumulatively increased downstream and maximized at the downstream seigyu (seigyu C), as supported by the LSPIV and propeller current meter flow measurements (Figs. 3, 4). Bed scour was supposed to be high at this location with increased flow velocity and bed shear stress (Pandey et al., 2017). One of the largest ponds developed around the seigyu units was at this location in early July (Figs. 6a, 7b). The maximum scour near the downstream seigyu contrasts with that reported in previous studies, in which maximum scour was observed near the upstream unit of multiple spur dykes arrayed streamwise in experimental or simulated straight channels (Zhang and Nakagawa, 2008; Pandey et al., 2017). The difference may be explained by the downstream seigyu being closer to the river middle, where the flow velocity was higher. Ponds also developed at the bank side of seigyu units, where flow diverted by the seigyu units passed through the space between two units (Fig. S2). A water level rise induced by the seigyu backwater and a water level difference between the stoss and lee sides of seigyu were evident during our survey. It is likely that the bank-side diverted flow plunged and induced downward flow and vertical vortices (Borg et al., 2007; Harrison and Keller, 2007; Pagliara and Kurdistani, 2017), resulting in bed scouring. The spatial distribution of TKE and its dissipation rate did not coincide with the location of erosion around seigyu. Different spatial scales (resolutions) may be required to further examine the relationship between TKE and bed changes.

The ponds around seigyu appeared to decrease in number and size with increasing flood water level. Although the ponds developed after floods in the early half of the survey period, they were filled by sediment after larger floods that occurred in the latter half of the period, and a single and small pond remained after the largest flood near seigyu. Notably, the responses of ponds differed for two similar-size floods in July (the floods before the 4th and 5th surveys); the ponds increased in the former but decreased in the latter. The floods differed in the duration of the falling limb of the hydrograph (Fig. 9a–b). Due to a modest decrease in the water level, seigyu units were inundated (shaded portion of the hydrograph in Fig. 9a and b) and thus affected the surrounding flow and bed for a longer time in the former flood than in the latter flood. It is likely that in the latter flood, sediment was delivered and deposited during the peak flow, and it remained afterwards because less time was available for sediment erosion in the falling limb period.

Fig. 6. Digital elevation map (DEM) for the 6 periods of the pond survey (a), and elevation changes between two consecutive periods (b) around the seigyu units. The location of the ponds was shown by white line. No pond occurred near the seigyu units in period 6.

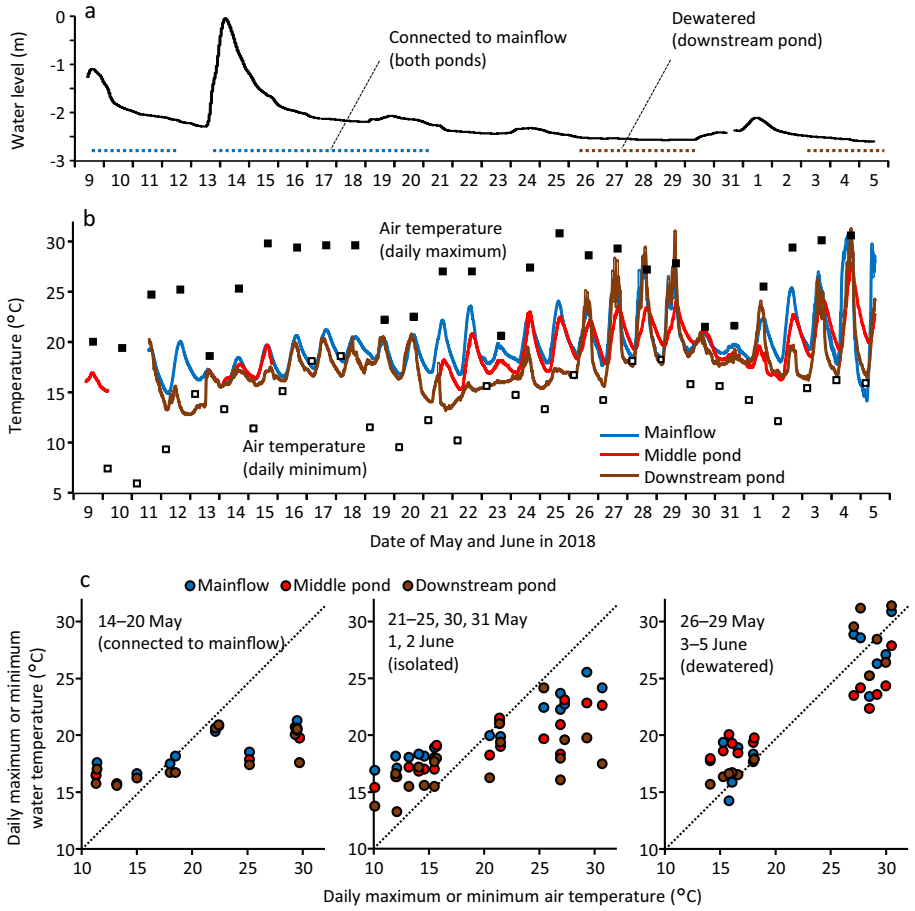

Fig. 8. Changes in the water level of the main flow (a) and water temperature in the ponds (b), and the relationship between the air and water temperatures (daily maximum and minimum values) for different water level stages (c) in late spring 2018. The line of equality is shown in (c).

The scouring effect of seigyu units does not always increase with increasing water level. Between the two floods that we measured to determine the surface flow velocity, the mean flow velocity around seigyu units was greater for the larger flood, whereas in addition to the spatial variation in flow velocity, the dissipation rate of TKE was greater for the smaller flood. The spatial variations in flow velocity and direction were amplified during the smaller flood because only one-third of the seigyu units were submerged, and the surface flow was blocked and deflected by the lower and wider parts of the seigyu structures. Flow convergence, flow separation, and plunging are considered to promote vertical mixing of water and production of vortices and upwells on the surface. In contrast, the seigyu units were almost fully submerged in the larger flood, and only the apex affected the surface flow. Although the flow behaviours of the middle and bottom layers in the water column were not visible, the spatial variation in flow velocity in these layers may be less amplified by the overlying surface layer during large floods. In addition, flow might have been more concentrated in the upper layer with less flow obstruction, and a smaller flow velocities and bed shear stress near the bottom might have induced deposition around the seigyu. Meanwhile, in the larger flood, the TKE and its dissipation rate were high beside the bank with an overhanging tree (Fig. 5a), where bed was scoured and eroded during the largest flood (between periods 5 and 6, Fig. 6). It seems that the flow deflected by the seigyu A and bank converged between them and promoted vertical turbulence and bed scouring.

Alternatively, it is assumed that it was in a “clear water” condition during partially submerged floods because of the overall low flow velocity and bed shear stress, and bed-load transport was only possible near the seigyu units where the flow velocity was high. In contrast, it was in a “live bed” condition during fully submerged floods due to overall high flow velocity and bed shear stress, and sand from upstream would be transported and deposited (trapped) around seigyu where flow velocity decreased.

In studies of spur dykes, it has often been reported that bed shear stress and scour hole depth decrease with increasing submergence ratio of the dykes (Rodrigue-Gervais et al., 2011; Mehraein et al., 2017; Pandey et al., 2017), which agrees with the decreased scour in fully submerged conditions. It is suspected that the scouring effect of seigyu increases with increasing water level up to a certain critical stage, up to which seigyu units sufficiently block and deflect flow, whereas it decreases with increasing water level over the critical stage. In addition, sediment transport from upstream is likely to increase with increasing discharge and may offset the bed scouring action of flow in high-flow stages.

Floods prior to each pond survey were re-evaluated in terms of the seigyu submergence level based on the submergence depth of seigyu units and the flood duration (i.e., shaded area in Fig. 9a–b) for three different submergence stages (zero to half submergence, half to full submergence, overtopped submergence) (Fig. 9c). The changes in submergence level in the two lower stages (Fig. 9c) corresponded well to the changes in the frequency and size of ponds (Fig. 7a–c), except for the lowest stage during the 6th survey. For this flood, the lowest submergence stage was relatively long, with a small flow rise before the main rise, and erosion that occurred during the small rise may have been offset by sediment deposition during the main rise. Excluding this small rise before the peak (hatched area in Fig. 9c), the submergence level was lower for the 6th survey than for the 3rd and 4th surveys, in which the frequency and size of ponds were at maximums (Fig. 7a–c). Because pond formation depends on the balance of erosion and deposition, the results may differ if sediment supply conditions change in different years and for different gravel bars. Further monitoring is needed to confirm the generality of our findings.

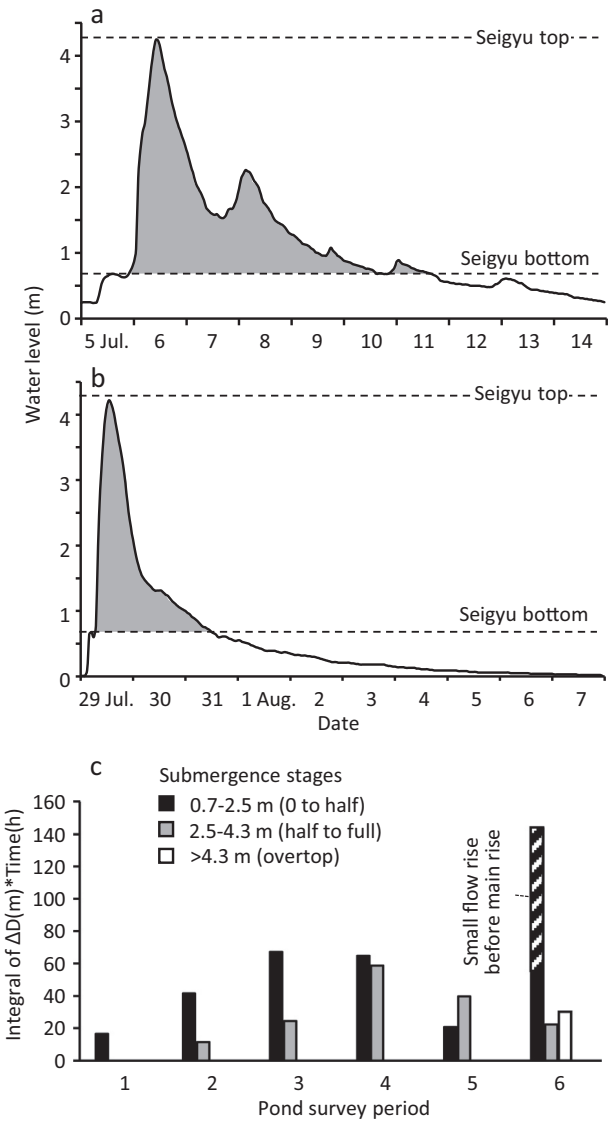

Fig. 9. Hydrographs of flood events in late July (a) and early August (b) and the seigyu submergence level based on the submersion depth and duration (shaded area in a and b) for floods prior to each survey time (c).

4.2. Water depth and thermo-features of ponds

There are few things to shade bed surfaces from sunlight on nonvegetated bars. Thus, the water temperature of ponds on such open bars is susceptible to air temperature fluctuations and heating by solar radiation (Brunke et al., 2003; Tonolla et al., 2010; Paillex et al., 2017), which can lead to lethal conditions for aquatic organisms. In this study, however, the diel temperature range was sometimes smaller for the ponds than for the main flow, at least for several days after isolation from the main flow (Fig. 8b). This relation is likely because the pond water upwelled from the hyporheic zone, in which the temperature is more stable than it is in the surface water zone (Arrigoni et al., 2008; Burkholder et al., 2008; Ock et al., 2015). Additionally, water turns over and buffers the effects of air temperature and solar radiation. During temperature monitoring with the logger, the deeper pond exhibited a moderate temperature cycle, which reflects the continuous supply of water from the hyporheic zone. The shallower pond sometimes exhibited an irregular fluctuation pattern, which may imply that the main source of water changed when the subsurface water level changed (e.g., from the deep to shallow hyporheic layers).

Because the dry bed surface of the bar often exceeded 50–60 °C on sunny days in mid-summer (personal observation), the ponds around seigyu were prone to be heated. Deeper ponds may provide buffering functions because the temperature of bars can rapidly decrease with sediment depth (Tonolla et al., 2010), or the water may originate from deep hyporheic layers with more stable temperatures (Marzadri et al., 2013; Cranswick et al., 2014). Deeper ponds also continue for a longer time and can support inhabitants because of the water supply from deeper layers, which remains even when the subsurface water table falls down. Our results support the assumption that bar ponds are fed by hyporheic water, which can buffer temperature fluctuations. Systematically designed surveys are needed to obtain clear assessments of the spatial and temporal heterogeneity in pond temperature.

Ponds on nonvegetated bars are often inhabited by species with high dispersal ability because they are frequently flooded and disturbed (Paillex et al., 2007; Skern et al., 2010). In ponds near seigyu, nearly 80 taxa of invertebrates and fish were recorded in 2018, including coleopteran (e.g., hydrophilid and elmid species) and hemipteran (corixid species) insect taxa that can tolerate relatively high temperatures (Tazumi et al., 2019, Fig. S3). More than 10 mayfly taxa (including *Thraulus*, a hyporheic zone inhabitant, Tabacchi et al., 1993) that are not adapted to high temperatures also occurred in these ponds. It is also known that ponds are important habitats for mayfly *Siphlonurus*, which were abundant in the study river, and other related species to migrate before emergence in early spring in temperate rivers (Gibbs and Mingo, 1986; Gibbs and Siebenmann, 1996). In addition, ponds developed underneath seigyu units can serve as refuges for small and juvenile fish that are not adapted to high temperatures, allowing these fish to escape from birds and larger fish. Thus, given that shallow ponds occur more frequently than deep ponds, not only the formation of bar ponds but also the formation of deep ponds that buffer temperature fluctuations are assumed to be the keys to enhancing habitat diversity and the colonization potential of various aquatic species.

5. Conclusion

The effects of the “seigyu”, traditional river training structures formerly used to protect riverbanks, on the restoration of floodplain habitats were monitored throughout a flood season. Spatial flow patterns around three seigyu units during floods were captured by a UAV, an image processing technique based on LSPIV, and flow turbulence evaluation. Beds were scoured, and bar ponds were developed where flow converged locally around seigyu units during floods. The development of ponds around these units was not always promoted by larger floods, and it is suggested that the bed scouring effect of seigyu units was most pronounced in flow stages in which the units were partially submerged. Our results support the assumption that bar ponds are fed by hyporheic water and that heating of water by direct sunlight is mitigated by the supply and turnover of hyporheic water. The formation of deep ponds and the sufficient hyporheic exchange of water are considered to be keys to enhancing the colonization of bar ponds by various aquatic species. Various studies are required in the future regarding the effect of the seigyu, including the detailed measurements of the vertical velocity profiles, water depth changes in the vicinity of the seigyu, local bed deposition changes associated with dimensional analysis of ponds, and the link between pond geometry and temperature.

CRediT authorship contribution statement

Sohei Kobayashi: Writing, Formal analysis, Conceptualization, editing. **Sameh A. Kantoush:** Conceptualization, Methodology, original draft, editing. **Mahmood M. Al-mamari:** Formal analysis, Investigation. **Masafumi Tazumi:** Investigation, Data curation. **Yasuhiro Takemon:** Supervision, Funding, Investigation. **Tetsuya Sumi:** Supervision.

Declaration of competing interest

The authors declare that they have no known competing financial interests or personal relationships that could have appeared to influence the work reported in this paper.

Acknowledgements

We thank the employees of the Yodogawa River Office, Ministry of Land, Infrastructure, Transport and Tourism, for providing valuable information and support throughout the field study. We also thank the students and researchers of the Socio- and Eco-Environment Risk Management, Disaster Prevention Research Institute (DPRI), Kyoto University, for helping with field surveys. Additionally, we thank Dr. Takahiro Koshiba of DPRI and Prof. Koichi Unami of Graduate School of Agriculture, Kyoto University for their support for flow turbulence calculations. This study was supported by JSPS KAKENHI (Grant Number JP21H01434) and River Works Technology Research and Development Program from Ministry of Land, Infrastructure, Transport and Tourism (Study of a riverbed management method for the Kizu River using traditional river works), Japan. This paper was also based on achievements of the collaborative research program (2021 W-01) of the Disaster Prevention Research Institute of Kyoto University. The manuscript was greatly developed by three anonymous reviewers. English was edited by American Journal Experts.

Appendix A. Supplementary data

Supplementary data to this article can be found online at https://doi.org/10.1016/j.scitotenv.2022.152992.

References

Al-mamari, M.M., Kantoush, S.A., Kobayashi, S., Sumi, T., Saber, M., 2019. Real-time measurement of flash-flood in a Wadi area by LSPIV and STIV. Hydrology 6, 27. https://doi.org/10.3390/hydrology6010027.

Amoros, C., 2001. The concept of habitat diversity between and within ecosystems applied to river side-arm restoration. Environ. Manag. 28, 805–817. https://doi.org/10.1007/s002670010263.

Amoros, C., Bornette, G., 2002. Connectivity and biocomplexity in waterbodies of riverine floodplains. Freshw. Biol. 47, 761–776. https://doi.org/10.1046/j.1365-2427.2002.00905.x.

Arrigoni, A.S., Poole, G.C., Mertes, L.A.K., O'Daniel, S.J., Woessner, W.W., Thomas, S.A., 2008. Buffered, lagged, or cooled? Disentangling hyporheic influences on temperature cycles in stream channels. Wat. Resour. Res. 44, W09418. https://doi.org/10.1029/2007WR006480.

Borg, D., Rutherfurd, I., Stewardson, M., 2007. The geomorphic and ecological effectiveness of habitat rehabilitation works: continuous measurement of scour and fill around large logs in sand-bed streams. Geomorphology 89, 205–216. https://doi.org/10.1016/j.geomorph.2006.07.027.

Bowen, Z.H., Bovee, K.D., Waddle, T.J., 2003. Effects of flow regulation on shallow-water habitat dynamics and floodplain connectivity. Trans. Am. Fish. Soc. 132, 809–823. https://doi.org/10.1577/T02-079.

Briggs, M.A., Lautz, L.K., McKenzie, J.M., Gordon, R.P., Hare, D.K., 2012. Using high-resolution distributed temperature sensing to quantify spatial and temporal variability in vertical hyporheic flux. Water Resour. Res. 48, WR011227. https://doi.org/10.1029/2011WR011227.

Brunke, M., Hoehn, E., Gonser, T., 2003. Patchiness of river–groundwater interactions within two floodplain landscapes and diversity of aquatic invertebrate communities. Ecosystems 6, 707–722. https://doi.org/10.1007/PL00021501.

Burkholder, B.K., Grant, G.E., Haggerty, R., Khangaonkar, T., Wampler, P.J., 2008. Influence of hyporheic flow and geomorphology on temperature of a large, gravel-bed river, Clackamas River, Oregon, USA. Hydrol. Process. 22, 941–953. https://doi.org/10.1002/hyp.6984.

Carré, D.M., Biron, P.M., Gaskin, S.J., 2007. Flow dynamics and bedload sediment transport around paired deflectors for fish habitat enhancement: a field study in the Nicolet River. Can. J. Civ. Eng. 34, 761–769. https://doi.org/10.1139/l06-083.

Choi, M., 2014. Studies on ecological evaluation of reach-scale channel configuration based on habitat structure and biodiversity relations. Kyoto University Doctoral dissertation.

Choi, M., Takemon, Y., Ikeda, K., Jung, K., 2018a. Relationships among animal communities, lentic habitats, and channel characteristics for ecological sediment management. Water 10, 1479. https://doi.org/10.3390/w10101479.

Choi, M., Takemon, Y., Yu, W., Jung, K., 2018b. Ecological evaluation of reach scale channel configuration based on habitat structures for river management. J. Hydroinform. 20, 622–632. https://doi.org/10.2166/hydro.2018.139.

Couto, T.B.A., Zuanon, J., Olden, J.D., Ferraz, G., 2018. Longitudinal variability in lateral hydrologic connectivity shapes fish occurrence in temporary floodplain ponds. Can. J. Fish. Aquat. Sci. 75, 319–328. https://doi.org/10.1139/cjfas-2016-0388.

Cranswick, R.H., Cook, P.G., Lamontagne, S., 2014. Hyporheic zone exchange fluxes and residence times inferred from riverbed temperature and radon data. J. Hydrol. 519, 1870–1881. https://doi.org/10.1016/j.jhydrol.2014.09.059.

Dole-Olivier, M.J., Wawzyniak, V., des Chatellier, M.C., Marmonier, P., 2019. Do thermal infrared (TIR) remote sensing and direct hyporheic measurements (DHM) similarly detect river-groundwater exchanges? Study along a 40 km-section of the Ain River (France). Sci. Total Environ. 646, 1097–1110. https://doi.org/10.1016/j.scitotenv.2018.07.294.

Feyrer, F., Sommer, T.R., Zeug, S.C., O'Leary, G., Harrell, W., 2004. Fish assemblages of perennial floodplain ponds of the Sacramento River, California (USA), with implications for the conservation of native fishes. Fish. Manag. Ecol. 11, 335–344. https://doi.org/10.1111/j.1365-2400.2004.00386.x.

Frissell, C.A., Liss, W.J., Warren, C.E., Hurley, M.D., 1986. A hierarchical framework for stream habitat classification: viewing streams in a watershed context. Env. Manag. 10, 199–214. https://doi.org/10.1007/BF01867358.

Gariglio, F.P., Tonina, D., Luce, C.H., 2013. Spatiotemporal variability of hyporheic exchange through a pool-riffle-pool sequence. Water Resour. Res. 49, 7185–7204. https://doi.org/10.1002/wrcr.20419.

Gergel, S.E., 2002. Assessing cumulative impacts of levees and dams on floodplain ponds: a neutral-terrain model approach. Ecol. Appl. 12, 1740–1754. https://doi.org/10.1890/1051-0761(2002)012[1740:ACIOLA]2.0.CO;2.

Gibbs, K.E., Mingo, T.M., 1986. The life history, nymphal growth rates, and feeding habits of Siphlonisca aerodromia Needham (Ephemeroptera: Siphlonuridae) in Maine. Can. J. Zool. 64, 427–430. https://doi.org/10.1139/z86-066.

Gibbs, K.E., Siebenmann, M., 1996. Life history attributes of the rare mayfly Siphlonisca aerodromia Needham (Ephemeroptera: Siphlonuridae). J. N. Am. Benthol. Soc. 15, 95–105.

Harper, D., Mekotova, J., Hulme, S., White, J., Hall, J., 1997. Habitat heterogeneity and aquatic invertebrate diversity in floodplain forests. Glob. Ecol. Biogeogr. Letters 6, 275–285. https://doi.org/10.2307/2997741.

Harrison, L.R., Keller, E.A., 2007. Modeling forced pool–riffle hydraulics in a boulder-bed stream, southern California. Geomorphology 83, 232–248. https://doi.org/10.1016/j.geomorph.2006.02.024.

Hawkins, C.P., Kershner, J.L., Bisson, P.A., Bryant, M.D., Decker, L.M., Gregory, S.V., McCullough, D.A., Overton, C.K., Reeves, G.H., Steedman, R.J., Young, M.K., 1993. A hierarchical approach to classifying stream habitat features. Fisheries 18, 3–12. https://doi.org/10.1577/1548-8446(1993)018<0003:AHATCS>2.0.CO;2.

Huryn, A.D., Wallace, J.B., 1987. Local geomorphology as a determinant of macrofaunal production in a mountain stream. Ecology 68, 1932–1942. https://doi.org/10.2307/1939884.

Jin, T., Liao, Q., 2019. Application of large scale PIV in river surface turbulence measurements and water depth estimation. Flow Meas. Instrum. 67, 142–152. https://doi.org/10.1016/j.flowmeasinst.2019.03.001.

Johnson, E.D., Cowen, E.A., 2017. Estimating bed shear stress from remotely measured surface turbulent dissipation fields in open channel flows. Water Resour. Res. 53, 1982–1996. https://doi.org/10.1002/2016WR018898.

Kani, T., 1981. Stream classification in "ecology of torrent-inhabiting insects" (1944): an abridged translation. Physiol. Ecol. Jpn. 18, 113–118.

Karaus, U., Alder, L., Tockner, K., 2005. "Concave islands": habitat heterogeneity of parafluvial ponds in a gravel-bed river. Wetlands 25, 26–37.

Kondolf, G.M., 1997. Hungry water: effects of dams and gravel mining on river channels. Env. Manag. 21, 533–551. https://doi.org/10.1007/s002679900048.

Marzadri, A., Tonina, D., Bellin, A., 2013. Effects of stream morphodynamics on hyporheic zone thermal regime. Water Resour. Res. 49, 2287–2302. https://doi.org/10.1002/wrcr.20199.

Mehraein, M., Ghodsian, M., Mashizi, M.K., Vaghefi, M., 2017. Experimental study on flow pattern and scour hole dimensions around a T-shaped spur dike in a channel bend under emerged and submerged conditions. Int. J. Civ. Eng. 15, 1019–1034. https://doi.org/10.1007/s40999-017-0175-x.

Nagayama, S., Nakamura, F., 2010. Fish habitat rehabilitation using wood in the world. Landscape Ecol. Eng. 6, 289–305. https://doi.org/10.1007/s11355-009-0092-5.

Nakamura, F., Seo, J.I., Akasaka, T., Swanson, F.J., 2017. Large wood, sediment, and flow regimes: their interactions and temporal changes caused by human impacts in Japan. Geomorphology 279, 176–187. https://doi.org/10.1016/j.geomorph.2016.09.001.

Negishi, J.N., Katsuki, K., Kume, M., Nagayama, S., Kayaba, Y., 2014. Terrestrialization alters organic matter dynamics and habitat quality for freshwater mussels (Unionoida) in floodplain backwaters. Freshwat. Biol. 59, 1026–1038. https://doi.org/10.1111/fwb.12325.

Nhiwatiwa, T., Brendonck, L., Waterkeyn, A., Vanschoenwinkel, B., 2011. The importance of landscape and habitat properties in explaining instantaneous and long-term distributions of large branchiopods in subtropical temporary pans. Freshwat. Biol. 56, 1992–2008. https://doi.org/10.1111/j.1365-2427.2011.02630.x.

Ock, G., Gaeuman, D., McSloy, J., Kondolf, G.M., 2015. Ecological functions of restored gravel bars, the Trinity River, California. Ecol. Eng. 83, 49–60. https://doi.org/10.1016/j.ecoleng.2015.06.005.

Pagliara, S., Kurdistani, S.M., 2017. Flume experiments on scour downstream of wood stream restoration structures. Geomorphology 279, 141–149. https://doi.org/10.1016/j.geomorph.2016.10.013.

Paillex, A., Castella, E., Carron, G., 2007. Aquatic macroinvertebrate response along a gradient of lateral connectivity in river floodplain channels. J. N. Am. Benthol. Soc. 26, 779–796. https://doi.org/10.1899/06-12.1.

Paillex, A., Castella, E., zu Ermgassen, P., Gallardo, B., Aldridge, D.C., 2017. Large river floodplain as a natural laboratory: non-native macroinvertebrates benefit from elevated temperatures. Ecosphere 8, e01972. https://doi.org/10.1002/ecs2.1972.

Pandey, M., Ahmad, Z., Sharma, P.K., 2017. Scour around impermeable spur dikes: a review. ISH J. Hydraul. Eng. 24, 25–44. https://doi.org/10.1080/09715010.2017.1342571.

Poole, G.C., 2002. Fluvial landscape ecology: addressing uniqueness within the river discontinuum. Freshwat. Biol. 47, 641–660. https://doi.org/10.1046/j.1365-2427.2002.00922.x.

Rodrigue-Gervais, K., Biron, P.M., Lapointe, M.F., 2011. Temporal development of scour holes around submerged stream deflectors. J. Hydraul. Eng. 137, 781–785. https://doi.org/10.1061/(ASCE)HY.1943-7900.0000353.

Roni, P., Beechie, T., Pess, G., Hanson, K., 2015. Wood placement in river restoration: fact, fiction, and future direction. Can. J. Fish. Aquat. Sci. 72, 466–478. https://doi.org/10.1139/cjfas-2014-0344.

Sheng, J., Meng, H., Fox, R.O., 2000. A large eddy PIV method for turbulence dissipation rate estimation. Chem. Eng. Sci. 55, 4423–4434. https://doi.org/10.1016/S0009-2509(00)00039-7.

Skern, M., Zweimüller, I., Schiemer, F., 2010. Aquatic heteroptera as indicators for terrestrialisation of floodplain habitats. Limnologica 40, 241–250. https://doi.org/10.1016/j.limno.2009.09.002.

Tabacchi, E., Decamps, H., Thomas, A., 1993. Substrate interstices as a habitat for larval Thraulus bellus (Ephemeroptera) in a temporary floodplain pond. Freshwat. Biol. 29, 429–439. https://doi.org/10.1111/j.1365-2427.1993.tb00777.x.

Tazumi, M., Kobayashi, S., Takemon, Y., Sumi, T., Takebayashi, H., Inagak, S., Kawauch, Y., Kato, Y., Nagatani, N., Yonekura, S., Yamaguchi, K., 2019. An application of Japanese traditional river works "Seigyu" for habitat restoration in the Kizu River. 14th International Symposium on River Sedimentation, September 16-19, 2019, Chengdu, China.

Tockner, K., Schiemer, F., Ward, J.V., 1998. Conservation by restoration: the management concept for a river-floodplain system on the Danube River in Austria. Aquat. Conserv. 8, 71–86. https://doi.org/10.1002/(SICI)1099-0755(199801/02)8:1<71::AID-AQC265>3.0.CO;2-D.

Tomino, A., 2002. Japanese traditional river training works [1], Shinzansha, Tokyo (In Japanese).

Tonolla, D., Acuna, V., Uehlinger, U., Frank, T., Tockner, K., 2010. Thermal heterogeneity in river floodplains. Ecosystems 13, 727–740. https://doi.org/10.1007/s10021-010-9350-5.

Trauth, N., Schmidt, C., Vieweg, M., Oswald, S.E., Fleckenstein, J.H., 2015. Hydraulic controls of in-stream gravel bar hyporheic exchange and reactions. Water Resour. Res. 51, 2243–2263. https://doi.org/10.1002/2014WR015857.

Van den Brink, F.W.B., Van der Velde, G., Wijnhoven, S., 2013. Diversity, occurrence and feeding traits of caddisfly larvae as indicators for ecological integrity of river-floodplain habitats along a connectivity gradient. Ecol. Indicat. 25, 92–98. https://doi.org/10.1016/j.ecolind.2012.09.010.

Zhang, H., Nakagawa, H., 2008. Scour around spur dike: recent advances and future researches. Ann. Disaster Prev. Res. Inst., Kyoto Univ. 51B, 633–652.

Zilli, F.L., Marchese, M.R., 2011. Patterns in macroinvertebrate assemblages at different spatial scales. Implications of hydrological connectivity in a large floodplain river. Hydrobiologia 663, 245–257. https://doi.org/10.1007/s10750-010-0576-1.